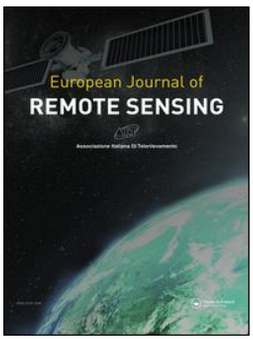

European Journal of Remote Sensing

ISSN: (Print) 2279-7254 (Online) Journal homepage: http://www.tandfonline.com/loi/tejr20

Impact of day/night time land surface temperature in soil moisture disaggregation algorithms

Miriam Pablos, María Piles, Nilda Sánchez, Mercè Vall-llossera, José Martínez-Fernández & Adriano Camps

To cite this article: Miriam Pablos, María Piles, Nilda Sánchez, Mercè Vall-llossera, José Martínez-Fernández & Adriano Camps (2016) Impact of day/night time land surface temperature in soil moisture disaggregation algorithms, European Journal of Remote Sensing, 49:1, 899-916

To link to this article: http://dx.doi.org/10.5721/EuJRS20164947

Published online: 17 Feb 2017.

European Journal of Remote Sensing - 2016, 49: 899-916
doi: 10.5721/EuJRS20164947
Received 04/02/2016 accepted 15/09/2016

European Journal of Remote Sensing
An official journal of the Italian Society of Remote Sensing

www.aitjournal.com

Impact of day/night time land surface temperature in soil moisture disaggregation algorithms

Miriam Pablos[1,4]*, María Piles[2,4], Nilda Sánchez[3], Mercè Vall-llossera[1,4], José Martínez-Fernández[3] and Adriano Camps[1,4]

[1]Universitat Politècnica de Catalunya (UPC) and Institut d'Estudis Espacials de Catalunya (IEEC), Campus Nord, buildings D3 and D4, 08034, Barcelona, Spain
[2]Institut de Ciències del Mar (ICM) and Consejo Superior de Investigaciones Científicas (CSIC), Passeig Marítim de la Barceloneta 37-49, 08003, Barcelona, Spain
[3]Instituto Hispanoluso de Investigaciones Agrarias (CIALE) and University of Salamanca (USAL), Duero 12, 37185, Villamayor, Salamanca, Spain
[4]Barcelona Expert Centre (BEC), Passeig Marítim de la Barceloneta 37-49, 08003, Barcelona, Spain
*Corresponding author, e-mail address: miriam.pablos@tsc.upc.edu

Abstract
Since its launch in 2009, the ESA's SMOS mission is providing global soil moisture (SM) maps at ~40 km, using the first L-band microwave radiometer on space. Its spatial resolution meets the needs of global applications, but prevents the use of the data in regional or local applications, which require higher spatial resolutions (~1-10 km). SM disaggregation algorithms based generally on the land surface temperature (LST) and vegetation indices have been developed to bridge this gap. This study analyzes the SM-LST relationship at a variety of LST acquisition times and its influence on SM disaggregation algorithms. Two years of *in situ* and satellite data over the central part of the river Duero basin and the Iberian Peninsula are used. *In situ* results show a strong anticorrelation of SM to daily maximum LST (R≈-0.5 to -0.8). This is confirmed with SMOS SM and MODIS LST Terra/Aqua at day time-overpasses (R≈-0.4 to -0.7). Better statistics are obtained when using MODIS LST day (R≈0.55 to 0.85; ubRMSD≈0.04 to 0.06 m^3/m^3) than LST night (R≈0.45 to 0.80; ubRMSD≈0.04 to 0.07 m^3/m^3) in the SM disaggregation. An averaged ensemble of day and night MODIS LST Terra/Aqua disaggregated SM estimates also leads to robust statistics (R≈0.55 to 0.85; ubRMSD≈0.04 to 0.07 m^3/m^3) with a coverage improvement of ~10-20 %.
Keywords: Disaggregation, downscaling, ensemble, SMOS, MODIS, REMEDHUS.

Introduction
Soil moisture (SM) is an essential climate variable that links the Earth's water and carbon cycles [GCOS, 2010]. SM regulates the energy exchange between the land and the atmosphere through the heat fluxes (latent and sensible) and its feedback on precipitation. Ultimately, SM affects the evolution of weather and climate [IPCC, 2014].

Nowadays, there are two space missions in orbit specifically devoted to measure the Earth's global surface SM using L-band radiometry: i) the Soil Moisture and Ocean Salinity (SMOS, 2009-2017) from the European Space Agency (ESA), and ii) the Soil Moisture Active Passive (SMAP, 2015-2018) from the U.S. National Aeronautics and Space Administration (NASA).

SMOS, launched on November 2, 2009, is the first L-band satellite dedicated to perform global measurements of surface SM [Kerr et al., 2010, 2016] and sea surface salinity [Font et al., 2010]. Its single payload is the Microwave Imaging Radiometer with Aperture Synthesis (MIRAS), an interferometric radiometer which provides multi-angular (0°-65°) and full-polarimetric (H, V, HV) observations with a spatial resolution of ~35-50 km [McMullan et al., 2008].

SMAP, launched on January 31, 2015, is the second L-band satellite specifically devoted to globally measuring surface SM and the freeze/thaw state of the soil [Entekhabi et al., 2010a; Chang et al., 2016]. It includes a real aperture radiometer and a Synthetic Aperture Radar (SAR), providing full-polarimetric observations at a single incidence angle (40°) with spatial resolutions of ~40 km and ~1-3 km, respectively [Entekhabi et al., 2014]. Unfortunately, the SMAP SAR ended its operations on July 7, 2015 due to a failure in the data transmission. The prospect use of the C-band SAR on-board of ESA's Sentinel 1 to provide the SMAP active-passive products is now being assessed [Leone, 2015].

The land surface temperature (LST) is also a key climate variable. Remotely sensed LST, acquired with thermal infrared (TIR) sensors, are routinely used in many operational applications, including weather forecasting. Polar orbiting satellites, such as Terra (1999-2020) and Aqua (2002-2020) missions provide LST measurements at high spatial resolution (1 km) with full global coverage (every 1-2 days), using the Moderate-Resolution Imaging Spectroradiometer (MODIS) [Wan and Snyder, 1999]. By contrast, geostationary satellites provide LST observations at a higher temporal resolution, but they have a continental coverage. The Spinning Enhanced Visible and InfraRed Imager (SEVIRI) sensor from the Meteosat Second Generation (MSG) mission (2002-2021) of ESA and European Organisation for the Explotation of Meteorological Satellites (EUMETSAT) provides frequent LST observations (every 15 minutes) over Europe with a spatial resolution of 3 km [Aminou et al., 1997]. However, MODIS Terra/Aqua is the only sensor providing daily LST measurements at the global scale. The local equatorial crossing times of SMOS, Terra and Aqua are approximately: 6:00/18:00 UTC for SMOS morning (ascending)/afternoon (descending) passes, 10:30/22:30 for Terra day (descending)/night (ascending) passes, and 13:30/1:30 for Aqua day (ascending)/night (descending) passes.

SM are LST are closely inter-related through soil emissivity, evapotranspiration and thermal inertia. Both SM and LST vary temporally, with the time of the day and the seasons, and spatially, with soil type and land cover [Seneviratne et al., 2010]. Recently, the SM-LST relationship and its influence on evapotranspiration were evaluated at the diurnal and seasonal scales. It was found that the daily maximum LST provided a better representation of the SM-LST covariability than the instantaneous LST [Pablos et al., 2016]. In this line, a previous study showed that SMOS Level 2 (L2) SM was more correlated to MODIS LST Terra/Aqua day than to LST night [Pablos et al., 2014]. The strongest correlation was also obtained when comparing SMOS Barcelona Expert Centre (BEC) Level 3 (L3) SM with MODIS LST Terra/Aqua day [Pablos et al., 2016].

Both SMOS and SMAP SM observations have a spatial resolution of ~40 km, which meets the needs of global scale applications, such as flood and drought monitoring, meteorological, ecological and hydrological model, and weather forecasting [Ochsner et al., 2013]. However, this spatial resolution is too coarse for regional and local scale studies. Due to that, there is a growing interest in developing techniques to enhance the spatial resolution of passive microwaves SM maps down to the ~1-10 km required. Different SMOS and SMAP pixel disaggregation algorithms have been proposed during the last decade. For SMOS, most approaches are based on the synergy of passive microwave with ancillary data obtained from optical visible/infrared (VIS/IR) observations [Piles et al., 2011, 2012, 2014, 2016; Merlin et al., 2012; Song and Jia, 2013; Fang and Lakshmi, 2014; Sánchez-Ruiz et al., 2014]. In these methods, the LST and the Normalized Difference Vegetation Index (NDVI) are fundamental input variables. In the case of SMAP, most approaches are based on the combination of active and passive data [Piles et al., 2009; Das et al., 2011; Guo et al., 2013; Das et al., 2014; Bruscantini et al., 2015].

Different studies have reported the emergence of a LST-Vegetation Index (VI) triangle or trapezoid space related to SM variations [Price, 1980; Carlson et al., 1994; Moran et al., 1994; Gillies and Carlson, 1995; Anderson et al., 1997; Sandholt et al., 2002; Anderson et al., 2007; Carlson, 2007; Stisen et al., 2008; Petropoulos et al., 2009]. Based on the LST-NDVI triangle, Piles et al. [2011] proposed a SMOS SM downscaling algorithm, using a linear regression model relating the coarse resolution SMOS SM and brightness temperature at horizontal polarization (T_{BH}) in a single incidence angle (θ_i=42.5º) with the higher spatial resolution MODIS LST and NDVI. The impact of using multi-angular and full-polarimetric information in this model was further evaluated in Piles et al. [2012]. Later, the algorithm was modified with a remarkable improvement in the model, including the brightness temperature at horizontal and vertical polarizations (T_{BH} and T_{BV}) and three incidence angles (θ_i=32.5º, 42.5º and 52.5º). The updated linear linking model for relating the variables across spatial scales can be expressed as [Piles et al., 2014]:

$$sm = a_0 + a_1 LST_N + a_2 NDVI_N + \sum_{i=1}^{3} a_{3i} T_{BH}(\theta_i)_N + \sum_{i=1}^{3} a_{4i} T_{BV}(\theta_i)_N \quad [1]$$

where a_0, a_1, a_2, a_{3i} and a_{4i} are the regression coefficients, sm stands for SM, LST_N is the normalized LST, $NDVI_N$ is the normalized NDVI, and $T_{BH}(\theta_i)_N$ and $T_{BV}(\theta_i)_N$ are the normalized horizontal and vertical polarized brightness temperatures, respectively, at incidence angles θ_i of 32.5º, 42.5º and 52.5º. The normalization of each variable X is performed for a specific morning/afternoon pass and scene, using:

$$X_N = \frac{X - X_{\min}}{X_{\max} - X_{\min}} \quad [2]$$

The use of NDVI and others VI from ShortWave InfraRed (SWIR) at different spatial (500 m vs. 1 km) and temporal (8 days *vs.* 16 days) resolutions in the model was also explored [Sánchez-Ruiz et al., 2014]. A recent review of the downscaling SM using passive

microwave data with VIS/IR information can be found in Piles and Sánchez [2016].
Nowadays, the approach of Piles et al. [2014] is the operational algorithm adopted by BEC to produce daily 1-km SM maps over the Iberian Peninsula as Level 4 (L4) SM products, which are freely distributed through its website: http://cp34-bec.cmima.csic.es. In its first version (SMOS BEC L4 SM v.1), the SMOS SM was combined with the closest MODIS LST acquisition, i.e.: SMOS morning (6:00 UTC) with MODIS Aqua night (1:30) or Terra day (10:30), and SMOS afternoon (18:00) with MODIS Aqua day (13:30) or Terra night (22:30). During their validation with ground-based data, the SMOS BEC L4 SM v.1 products showed better temporal correlation at the afternoon passes (R_{Terra}≈0.37 to 0.78; R_{Aqua}≈0.49 to 0.73) than at the morning passes (R_{Terra}≈0.30 to 0.70; R_{Aqua}≈0.31 to 0.64). Combining the two passes, higher correlations were achieved when using LST Terra than when using LST Aqua. Then, the use of LST Terra day was set as baseline. Nevertheless, since results from downscaled SM maps using LST Aqua were broadly consistent to those obtained with LST Terra, they were also used in operations when LST Terra was not available, i.e. masked by clouds [Piles et al., 2014].
In a SMOS L2 SM validation study with the same ground data used in Piles et al. [2014], no differences were detected when using the time-overpass or the daily average of *in situ* SM in the validation [Sánchez et al., 2012]. This indicates that a unique SM value per day could be representative of the entire day, except when rainfall events occur. Under these circumstances, and assuming that the spatial pattern of SM is persistent for a few hours before and after the SMOS pass [Martínez-Fernández and Ceballos, 2003], both SMOS SM morning and afternoon passes could be combined with any MODIS LST of the same day in the SM disaggregation algorithm. This fact, together with results obtained in Pablos et al. [2014, 2016], leaded to the production of a new release of downscaled SMOS SM maps over the Iberian Peninsula (SMOS BEC L4 SM v.2) using the MODIS LST Aqua day both for morning and afternoon passes.
Additionally, an ensemble created from the average of several disaggregated SM estimates (i.e., from all possible SMOS SM morning/afternoon and MODIS LST Terra/Aqua day/night combinations) could allow for improved coverage in presence of clouds, which masks MODIS LST observations. In this regard, different combinations of available SMOS morning and afternoon passes with 3 days of MODIS Terra and Aqua day time images were composited into an averaged downscaled SM, as a first step towards increasing the spatio-temporal coverage in SM data [Merlin et al., 2012]. Alternatively, the synergy of microwaves (SMOS) and geostationary optical IR data (MSG SEVIRI) was recently assessed to enhance the temporal and the spatial resolution of SM estimates [Piles et al., 2016].
This study analyzes the temporal correlation between SM and LST at different spatial scales, using two years (2012-2013) of *in situ* and space-borne observations. The main objective is to analyze the influence of the LST acquisition time in SM disaggregation algorithms and obtain the best LST-derived parameter to be used in SM downscaling. Firstly, the relationship between ground-based measurements of SM and LST from the Soil Moisture Measurement Stations Network of the University of Salamanca (REMEDHUS) [Sánchez et al., 2012] is assessed. Later, the relationship between remotely sensed SM and LST from SMOS and MODIS, respectively, over the REMEDHUS region and over the Iberian Peninsula is analyzed. The performance of all possible SMOS SM-MODIS LST combinations is evaluated separately. Also, the performance of an averaged ensemble of

downscaled SM datasets is compared to the downscaled SM using only MODIS LST Aqua day (the current approach of the SMOS BEC L4 SM v.2 products).

Data and methods

REMEDHUS data

The REMEDHUS network is located at the central part of the river Duero basin, in Spain, covering a semi-arid continental-Mediterranean agricultural region of 35 x 35 km [41.1-41.5 ºN, 5.1-5.7 ºW], with an area of ~1300 km^2. It is a member of the International Soil Moisture Network (ISMN, http://ismn.geo.tuwien.ac.at) and includes 21 permanent stations providing hourly SM and LST measurements in the top 5 cm of the soil. Both observations are acquired with Hydra Probes sensors, which measure with an accuracy of 0.003 m^3/m^3 and 0.6 ºC. The main land uses in REMEDHUS during the study period are vineyard (stations E10, F6, H7, I6, J3, and L3) with the lowest SM content, rainfed cereals or fallow (stations F11, H13, J12, J14, K4, K9, K10, K13, L7, M5, M9, N9, and O7) with an intermediate SM content, and forest-pasture (stations H9 and M13) with the highest SM content. The SM and LST measurements from stations placed in irrigated crops (K9 in 2012 and K13 in 2013) have been removed from the dataset.

SMOS data

This study uses the SMOS BEC L3 SM v.1 products, which are produced and freely distributed by BEC. They are obtained by quality-filtering and re-gridding the operational ESA SMOS L2 v.5.51 products. Grid points affected by radio frequency interferences (RFI) and/or SM with a Data Quality Index (DQX, defined as the error standard deviation) greater than 0.07 m^3/m^3 are discarded. A DQX-inverse weighted average is applied to bin the data from its native Icosahedral Snyder Equal Area (ISEA 4H9) grid to the global cylindrical 25-km Equal-Area Scalable Earth (EASE) grid. More details are available in BEC Team [2015]. A comprehensive validation of these products using two complementary small-scale and large-scale *in situ* networks and a surface water balance model can be found in González-Zamora et al. [2015].

MODIS data

The MODIS LST v.5 products from Terra (MOD11A1) and Aqua (MYD11A1) are provided by the U.S. Land Processes Distributed Active Archive Center (LP DAAC, https://lpdaac.usgs.gov). They have 1 km of spatial resolution and a nominal accuracy of 1°C under clear sky conditions. Higher errors (from 4ºC to 10°C) are reported in presence of clouds and heavy aerosols.

Methodology

In order to mimic the SMOS SM measurements, *in situ* SM acquired during SMOS morning and afternoon time-overpasses over the REMEDHUS region have been averaged. Additionally, *in situ* LST data have been considered at a variety of acquisition times: i) instantaneous T_i, ii) daily mean $\overline{T}$, iii) daily median T_{med}, iv) daily maximum T_{max}, v) daily minimum T_{min}, and vi) diurnal range $\Delta T = T_{max} - T_{min}$.

The 25-km SMOS BEC L3 SM and the 1-km MODIS LST pixels over the REMEDHUS

network and the Iberian Peninsula have been used in this study. In the case of MODIS LST, the two satellite platforms and time-passes are considered, i.e.: Terra day, Terra night, Aqua day, and Aqua night. The 1-km MODIS LST pixels have been aggregated to the 25-km EASE grid. Their values have been obtained as the mean of all 1-km pixels that fall within the corresponding 25-km cell. Later, LST values lower than -5ºC have been discarded from the study to avoid frozen soil conditions. Finally, a 3-day averaging window has been applied to SMOS and MODIS in order to reduce noise in the measurements. In the analysis over the Iberian Peninsula, all 25-km EASE pixels with its center at less than 0.15º of geometric distance from the coast have been removed to avoid sea-land contamination effects. The temporal correlation (R) of SM and LST has been evaluated using: i) *in situ* SM and LST from the REMEDHUS network, ii) space-borne SMOS SM and MODIS LST over the REMEDHUS area, and iii) space-borne SMOS SM and MODIS LST over the Iberian Peninsula. In all cases, non-significant correlations at the 95% of significance (ρ_{value}>0.05) are removed. Correlations computed with less than 10 coincident SM and LST measurements along the two years have also been discarded.

To assess the impact of using LST Terra or Aqua day/night time, all possible SMOS-MODIS combinations (SM morning/afternoon and LST Terra day/Terra night/Aqua day/Aqua night) have been used to produce eight datasets of 1-km disaggregated SM maps over the Iberian Peninsula (four datasets for SMOS morning and four datasets for SMOS afternoon passes). An averaged ensemble of the four downscaled datasets has also been produced for SMOS morning and afternoon passes, respectively. All of these downscaled SM estimates have been validated. To do so, the *in situ* SM value has been compared with the co-located SM estimate at each REMEDHUS station, using as statistical scores [Entekhabi et al., 2010b]: i) the standard deviation (std), ii) the correlation (R), iii) the unbiased Root Mean Square Difference (ubRMSD), iv) the bias, and v) the slope (*s*) estimated from a robust linear regression. The number of days of coverage along two years (*N*) has also been analyzed. The same statistics are also obtained at the network scale. They have been computed after averaging all stations of the downscaled SM estimates.

Results and discussion

Temporal correlation analysis

The correlation of *in situ* SM measured at the SMOS morning and afternoon passes and LST from the REMEDHUS network for a variety of acquisition times is shown in Figure 1. As expected, SM and LST are generally anticorrelated. These negative values of R mean that an increase in SM is related to a decrease in LST, and *vice versa*. There is a single outlier (depicted with a red cross) with a very low positive correlation (R≈0.1 to 0.2) corresponding to H7, an extremely dry vineyard station, with a SM ranging from 0 to 0.07 $m^3 \cdot m^{-3}$ along the two years. Analyzing the different LST acquisition times and considering the 25th and 75th percentiles (edges of the box) and the median (red central mark), the strongest correlation is obtained for the daily maximum LST (R_{Tmax}≈-0.49 to -0.76/-0.47 to -0.74 for morning/afternoon passes; -0.67/-0.61 in median). This is due to the fact that the time of T_{max} is also the time of maximum potential evapotranspiration, i.e., when there is a higher atmospheric demand for water. The weakest correlation is obtained for the LST diurnal range ($R_{\Delta T}$≈-0.49 to -0.66/-0.39 to -0.63; -0.57/-0.57 in median). The correlation obtained for the instantaneous LST (R_{Ti}≈-0.38 to -0.70/-0.52 to -0.74; -0.64/-0.61 in median) is very similar to the obtained

for T_{max} at the afternoon. This could be due to T_i values being closer (in time) to T_{max} at the afternoon passes than at the morning passes. In addition, the correlation obtained for the daily mean LST ($R_{\bar{T}}$≈-0.45 to -0.74/-0.45 to -0.71; -0.66/-0.60 in median) and for the daily median LST (R_{Tmed}≈-0.44 to -0.74/-0.43 to -0.70; -0.66/-0.59 in median) is slightly worse than the obtained for T_{max}, but slightly better than the obtained for T_i. The correlation obtained for daily minimum LST (R_{Tmin}≈-0.38 to -0.70/-0.42 to -0.70; 0.64/-0.60 in median) is also lower than those obtained for T_{max} and T_i. Overall results indicate that T_{max} could be an appropriate temperature for SM downscaling, as an alternative to T_i.

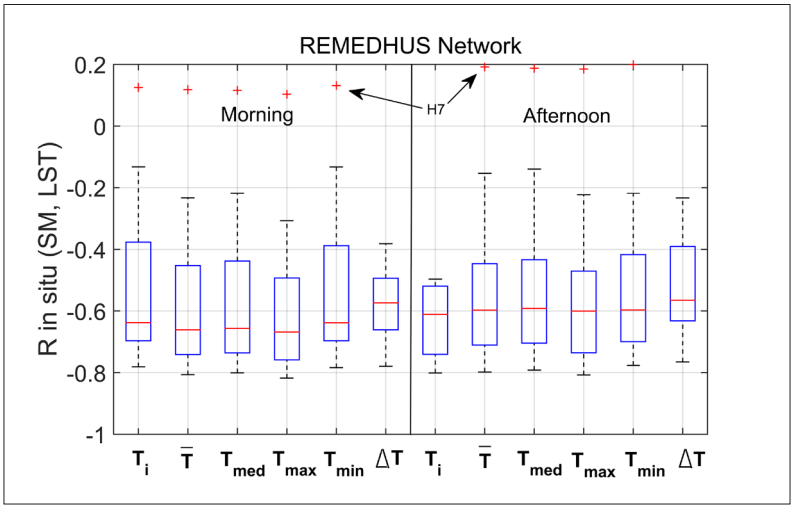

Figure 1 - Correlation (R) of *in situ* SM measured at the SMOS morning and afternoon passes and LST from the REMEDHUS network for a variety of acquisition times: i) instantaneous T_i, ii) daily mean $\overline{T}$, iii) daily median T_{med}, iv) daily maximum T_{max}, v) daily minimum T_{min}, and vi) diurnal range $\Delta T=T_{max}-T_{min}$.

The correlation of space-borne SMOS SM at morning and afternoon passes and all available MODIS LST over the REMEDHUS region (top) and the Iberian Peninsula (bottom) is presented in Figure 2. Note the low variability of R in REMEDHUS due to this region only covers four 25-km EASE pixels in the analysis. The strongest correlation is obtained for LST day times ($R_{Terra\ day}$≈-0.61/-0.62 in median for morning/afternoon passes; $R_{Aqua\ day}$≈-0.64/-0.67) and the weakest for LST night times ($R_{Terra\ night}$≈-0.47/-0.50; $R_{Aqua\ night}$≈-0.38/-0.41). This can be explained by the fact that LST day is closer (in time) to T_{max} than LST night, in agreement with results derived from the *in situ* analysis. The same behavior is observed over the Iberian Peninsula ($R_{Terra\ day}$≈-0.55/-0.56 in median for morning/afternoon passes; $R_{Terra\ night}$≈-0.44/-0.46; $R_{Aqua\ day}$≈-0.55/-0.58; $R_{Aqua\ night}$≈-0.41/-0.43). A possible reason for this behavior could be that MODIS LST at day time captures the spatial variability induced by topography that is not captured at night time. However, the correlation for the Iberian Peninsula is lower than for the REMEDHUS network, probably due to the presence of diverse climatic areas, which produces a major variability of R. Note that similar results are obtained at morning and afternoon passes, and using Terra or Aqua. In view of these results,

MODIS LST Terra day or Aqua day could be the most appropriate parameters to be used in the SMOS SM downscaling, both for morning and afternoon passes.

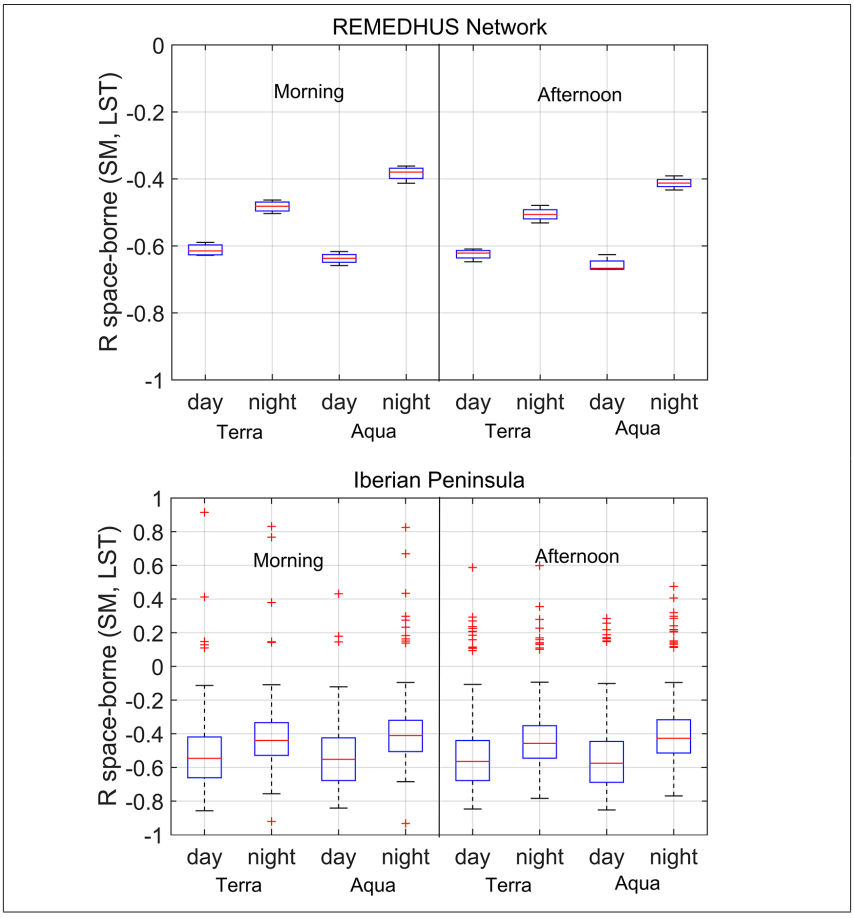

Figure 2 - Correlation (R) of space-borne SMOS SM at morning and afternoon passes and MODIS LST Terra day, Terra night, Aqua day, and Aqua night over the REMEDHUS region (top) and the Iberian Peninsula (bottom).

Figure 3 displays four correlation maps of space-borne SMOS SM at morning passes over the Iberian Peninsula and MODIS LST Terra day (top left), Terra night (top right), Aqua day (bottom left), and Aqua night (bottom right). Note that the correlation is strongest using LST day than night, both for Terra and Aqua, in agreement with results from Figure 2. Additionally, it can be observed that the spatial patterns of the correlation are similar both in day and night, with strong values in the South-Western part of the Peninsula, and weak values in the North-Western and Eastern parts. These maps of R show similar spatial patterns to those observed from the soil texture map of the Iberian Peninsula from the ECOCLIMAP database [Masson et al., 2003]. This suggests a possible relation with soil texture, which is used in the SMOS SM retrievals. However, further research is

needed to explore this hypothesis. When aggregating pixels by land cover, no significant differences in correlation are obtained among the different classes. Similar maps of R are obtained for SMOS afternoon passes (not shown). Since the daily maximum LST is not available from MODIS, the results support the use of MODIS LST Terra day or Aqua day in SM downscaling over the Iberian Peninsula. Other regions should be studied to confirm this result over different climates in the globe.

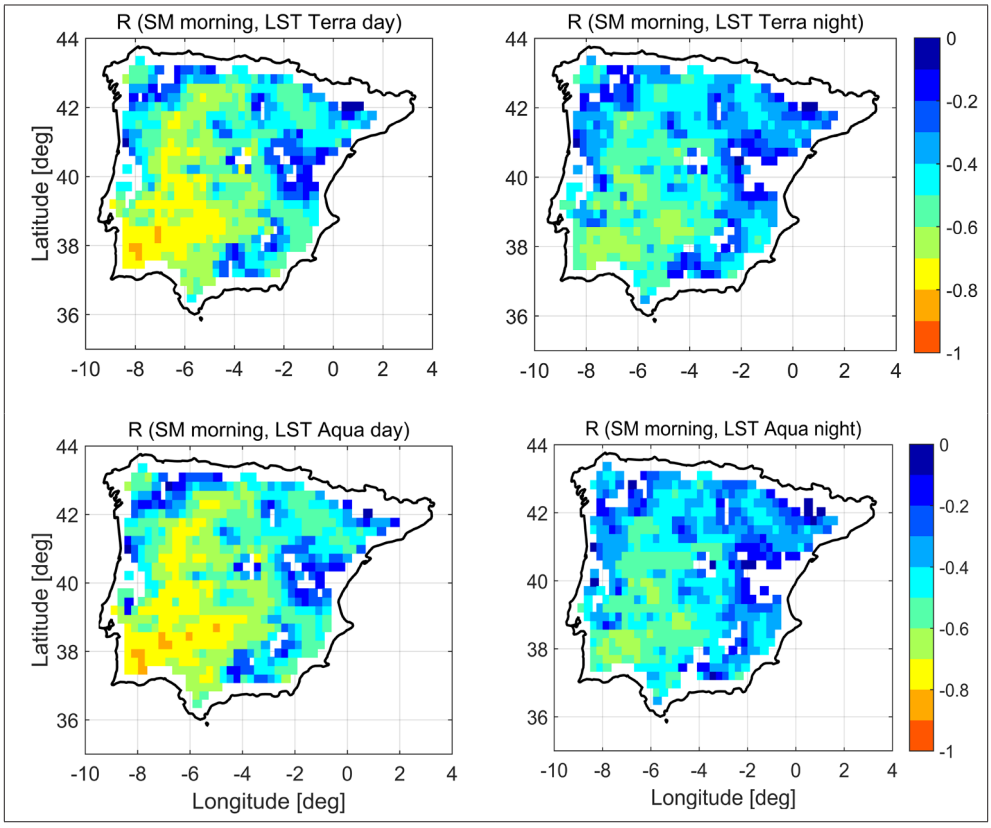

Figure 3 - Correlation (R) maps of space-borne SMOS SM at morning passes over the Iberian Peninsula and MODIS LST Terra day (top left), Terra night (top right), Aqua day (bottom left), and Aqua night (bottom right). Similar maps of R are obtained for SMOS afternoon passes (not shown).

Validation of disaggregated SM estimates

Taylor diagrams from the validation of 1-km disaggregated SM estimates using all MODIS LST Terra/Aqua day/night for SMOS morning (top) and afternoon (bottom) passes at each REMEDHUS station are shown in Figure 4. The standard deviation (std) of the reference (depicted with a star) has been computed from the average SM of the 21 REMEDHUS stations at SMOS morning and afternoon passes, respectively. In these diagrams, the ubRMSD is measured with the dashed line circles around the reference, the std is measured with the pointed line arches, and the correlation is measured with radial lines (not shown).

In general, the disaggregated SM products show higher correlation and lower ubRMSD when using Terra day or Aqua day (R≈0.55 to 0.85; ubRMSD≈0.04 to 0.06 m^3/m^3) than when using Terra night and Aqua night day (R≈0.45 to 0.80; ubRMSD≈0.04 to 0.07 m^3/m^3). Note that station H7 exhibits a higher error (ubRMSD≈0.08 m^3/m^3) and a lower correlation (R≈0.3) for all MODIS LST than the other stations, in agreement with results from Figure 1. Similar results are obtained for morning and afternoon passes. In view of these results, the use of MODIS LST day times is recommended for producing downscaled SMOS SM estimates, independently of the platform (Terra or Aqua satellites) and the SMOS time-overpass (morning or afternoon).

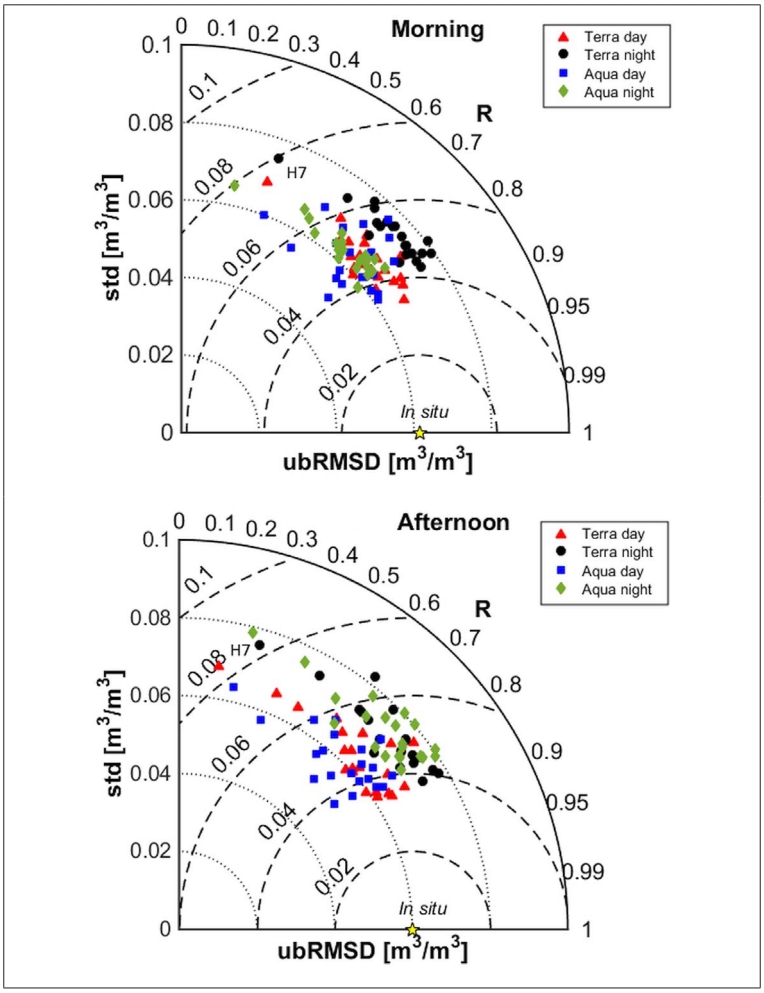

Figure 4 - Taylor diagrams from the validation of 1km-disaggregated SM estimates using MODIS LST Terra day (red triangles), Terra night (black circles), Aqua day (blue squares), and Aqua night (green diamonds) for each REMEDHUS station at the SMOS morning (top) and afternoon (bottom) passes.

Coverage improvement analysis

Scatter plots of correlation, ubRMSD and bias derived from the validation of downscaled SM when using MODIS LST Aqua day in the disaggregation algorithm (the operational SMOS BEC L4 SM v.2 product), and the averaged ensemble are shown in Figure 5. Note that the correlation (top left) is similar for both datasets. Regarding the ubRMSD (top right), it is clearly seen that there is a higher ubRMSD for the ensemble than for the downscaled SM using LST Aqua day. The bias (bottom) is similar, considering both SM estimates. These results indicate that both estimates compare well with *in situ* data. Nevertheless, there is a lower ubRMSD when MODIS LST Aqua day is used in the SM disaggregation algorithm.

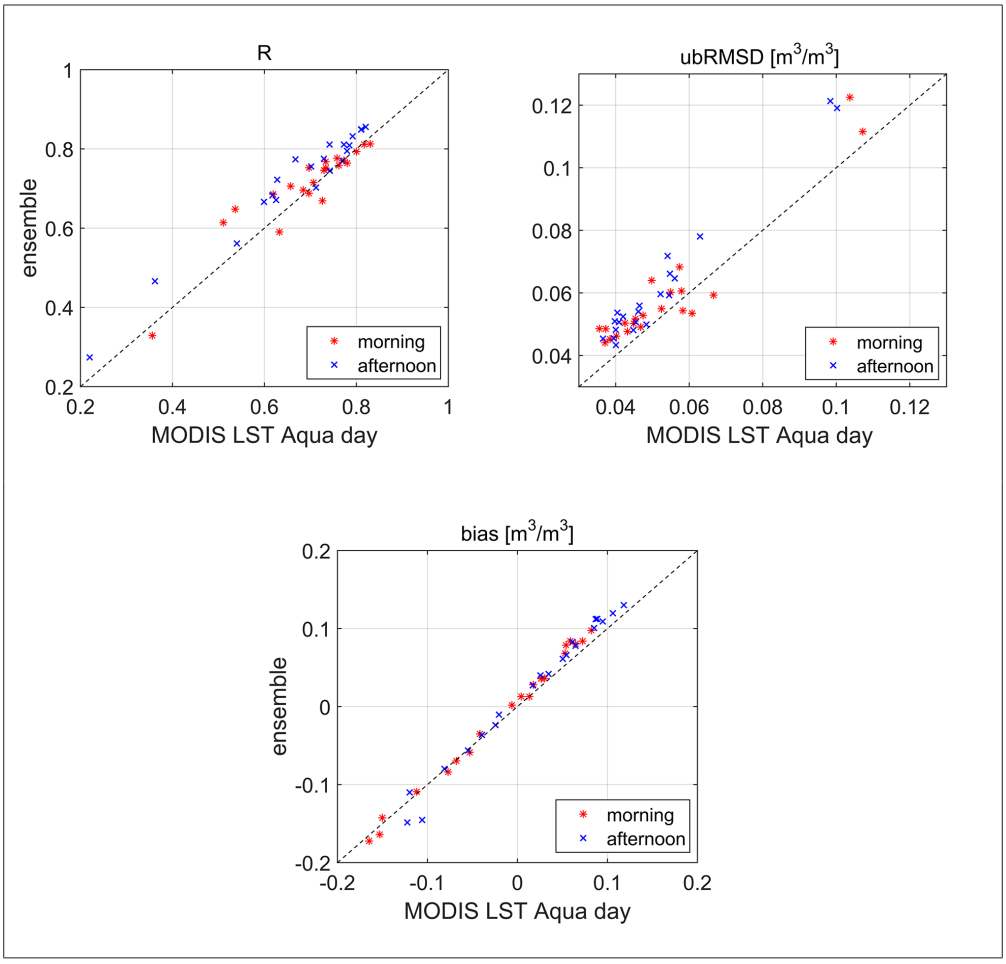

Figure 5 - Correlation (R, top left), unbiased Root Mean Square Difference (ubRMSD, top right), and bias (bottom) from the validation of downscaled SM when using MODIS LST Aqua day (the SMOS BEC L4 SM v.2 product), and the averaged ensemble at the SMOS morning (red asterisks) and afternoon (blue crosses) passes.

Table 1 - Correlation (R), unbiased Root Mean Square Difference (ubRMSD), bias, slope (*s*), and days of coverage along two years (*N*) from the validation of downscaled SM when using LST Aqua day in the disaggregation algorigthm (the SMOS BEC L4 SM v.2 product), and the averaged ensemble at the SMOS morning passes. Similar results are obtained at the SMOS afternoon passes (not shown).

Station	MODIS LST Aqua day					Averaged ensemble				
	R	ubRMSD [m³/m³]	bias [m³/m³]	s	N [days]	R	ubRMSD [m³/m³]	bias [m³/m³]	s	N [days]
E10	0.70	0.06	0.07	1.56	179	0.75	0.05	0.08	1.57	306
F6	0.78	0.04	-0.04	0.82	194	0.76	0.05	-0.04	0.96	323
F11	0.82	0.04	0.03	0.97	176	0.81	0.05	0.04	1.08	311
H7	0.36	0.06	0.05	1.48	175	0.33	0.07	0.08	1.93	319
H9	0.73	0.11	-0.15	0.38	155	0.75	0.11	-0.16	0.33	303
H13	0.68	0.05	-0.01	0.79	177	0.70	0.05	0.00	0.93	310
I6	0.51	0.05	0.06	1.42	167	0.61	0.06	0.08	2.79	322
J3	0.63	0.05	0.08	1.59	179	0.59	0.06	0.10	1.53	325
J12	0.80	0.04	-0.15	0.87	171	0.79	0.04	-0.14	0.93	317
J14	0.73	0.04	0.03	0.86	170	0.75	0.05	0.04	1.03	310
K4	0.62	0.06	0.06	1.92	194	0.69	0.06	0.08	2.21	329
K9	0.76	0.04	0.03	1.24	165	0.76	0.05	0.04	1.14	311
K10	0.83	0.04	0.05	1.40	165	0.81	0.05	0.07	1.44	320
K13	0.54	0.07	-0.11	0.43	190	0.65	0.06	-0.11	0.63	335
L3	0.70	0.04	0.02	1.21	179	0.69	0.05	0.03	1.32	310
L7	0.77	0.05	-0.08	0.53	202	0.77	0.05	-0.08	0.58	335
M5	0.66	0.06	0.00	1.12	184	0.71	0.05	0.01	1.19	324
M9	0.71	0.05	-0.07	0.56	161	0.71	0.05	-0.07	0.70	313
M13	0.73	0.10	-0.16	0.30	200	0.67	0.12	-0.17	0.30	333
N9	0.76	0.05	-0.05	0.64	193	0.78	0.05	-0.06	0.68	331
O7	0.73	0.04	0.01	0.67	170	0.77	0.05	0.01	0.74	324
Network	0.76	0.05	0.00	1.05	278	0.77	0.05	0.00	1.04	385

The correlation (R), ubRMSD, bias, slope (*s*), and days of coverage along two years (*N*) from the validation of downscaled SM when using MODIS LST Aqua day in the disaggregation algorithm (the SMOS BEC L4 SM v.2 product), and the averaged ensemble, are summarized in Table 1 for each station and for the entire network at the SMOS morning passes. The correlation is similar in both cases at the station scale ($R_{Aqua\ day}$≈0.36 to 0.83; $R_{ensemble}$≈0.36 to 0.83) and at the network scale ($R_{Aqua\ day}$≈0.76; $R_{ensemble}$≈0.77), in agreement with results of Figure 5. The ubRMSD is lower when using LST Aqua day than for the ensemble in the stations ($ubRMSD_{Aqua\ day}$≈0.04 to 0.10 m³/m³; $ubRMSD_{ensemble}$≈0.04 to 0.12 m³/m³), but they are equal considering the network average (ubRMSD≈0.05 m³/m³). The bias is similar

at the station scale (bias$_{\text{Aqua }day}$≈-0.15 to 0.08 m^3/m^3; bias$_{ensemble}$≈-0.17 to 0.10 m^3/m^3) and is also equal at the network scale (bias≈0.00 m^3/m^3). The slope is closer to 1 (ideal value) in the case of using LST Aqua day at the station scale ($s_{Aqua\ day}$≈0.30 to 1.92; $s_{ensemble}$≈0.30 to 2.79), but it is very similar considering the network ($s_{Aqua\ day}$≈1.05; $s_{ensemble}$≈1.04). However, there is an important coverage increase (~10-20 %) in the averaged ensemble taking into account the stations ($N_{Aqua\ day}$≈155 to 202 days, corresponding to ~25 % of coverage along two years; $N_{ensemble}$≈303 to 335 days, ~45 %) and considering the network average ($N_{Aqua\ day}$≈278 days, ~40 %; $N_{ensemble}$≈385 days, ~50 %). In both cases, H9 and M13 exhibit a differential behavior, with a higher ubRMSD (from 0.10 to 0.12 m^3/m^3) and bias (from -0.15 to -0.17 m^3/m^3) than the rest of the stations, and a very low slope (s≈0.30 to 0.38). These stations have a forest-pasture land use and are located in valley bottoms and flooded-prone areas, which could explain these differences. Additionally, H7 displays a very low correlation ($R_{Aqua\ day}$≈0.36; $R_{ensemble}$≈0.33). This agrees with results obtained in Figures 1 and 4, where H7 behaves as an outlier. Station K4 presents a high slope in both cases ($s_{Aqua\ day}$≈1.92; $s_{ensemble}$≈ 2.21). A possible reason for this may be the change of land use with respect to the previous years 2010 and 2011, when it was vineyard. Similar results are obtained using the SMOS afternoon passes (not shown).

Conclusions

This study presents a temporal correlation analysis between SM and LST using two years (2012-2013) of *in situ* data from the REMEDHUS network, and remotely sensed data from SMOS and MODIS, acquired over two study regions: the REMEDHUS network in the central part of the river Duero basin, and the Iberian Peninsula. This analysis helped us to better understand the SM-LST relationship at a variety of LST acquisition times and spatial scales. Also, several LST estimates were used as input of a SMOS-MODIS disaggregation algorithm, using all possible combinations of SMOS SM morning/afternoon-MODIS LST Terra/Aqua day/night, and producing eight 1-km disaggregated SM estimates.

In general, SM and LST are anticorrelated. Results obtained from the *in situ* analysis show that there is a stronger correlation between the SM and the daily maximum LST (R_{Tmax}≈-0.5 to -0.8), than for the other LST-derived parameters, such as the instantaneous LST, daily mean LST, daily median LST, daily minimum LST and LST diurnal range. This could be due to the fact that the time of maximum LST corresponds to the time of maximum potential evapotranspiration, and thus the time of a higher atmospheric demand of water. In this regard, the daily maximum LST can be an appropiate temperature for SM downscaling, as an alternative of using the instantaneous LST. No significant differences were obtained when using morning and afternoon passes.

Results from space-borne SMOS SM and MODIS LST Terra/Aqua day/night analysis show that there is a stronger correlation of SM to LST day than night, in both Terra and Aqua platforms over the REMEDHUS network (R_{day}≈-0.6 to -0.7; R_{night}≈-0.4 to -0.5) and over the Iberian Peninsula (R_{day}≈-0.4 to -0.7; R_{night}≈-0.3 to -0.6). This is consistent with the *in situ* analysis, since MODIS LST Terra/Aqua day is closer in time to the daily maximum LST than MODIS LST Terra/Aqua night. Also, correlation maps over the Iberian Peninsula display similar spatial patterns for LST day and for LST night times. Similar results are obtained for SMOS morning and afternoon passes. In view of these results, the use of MODIS LST Aqua day or Terra day is recommended for passive microwave SM downscaling.

A validation of eight 1-km disaggregated SM estimates with *in situ* data from the REMEDHUS network was performed. Better statistics (higher correlation and lower ubRMSD) are obtained when using MODIS LST Terra/Aqua day in the disaggregation than when using MODIS LST Terra/Aqua night, independently of the SMOS time-overpass (morning or afternoon). This agrees with results derived from the correlation analysis. Differences between the two platforms (Terra or Aqua) are negligible. This also supports the use of MODIS LST Terra/Aqua day for SMOS SM downscaling.

An averaged ensemble of four downscaled SM datasets (using all available MODIS LST) was proposed to improve the spatio-temporal coverage of the downscaled SM product with respect to a downscaled SM using MODIS LST Aqua day (the operational SMOS BEC L4 SM v.2 product). The two products exhibit a similar correlation ($R \approx 0.4$ to 0.8) and bias ($\approx$-0.17 to 0.10 $m^3 \cdot m^{-3}$) when compared to *in situ*. However, results show a lower ubRMSD and slopes closer to 1 when using MODIS LST Aqua day in the disaggregation (ubRMSD$\approx$0.04 to 0.10 $m^3 \cdot m^{-3}$ $s \approx 0.30$ to 1.92) than in the ensemble (ubRMSD$\approx$0.04 to 0.12 $m^3 \cdot m^{-3}$; $s \approx 0.30$ to 2.79). By constrast, there is a coverage increase of ~10 % at the station scale and ~20 % at the network scale. Therefore, an ensemble composed of an average of all available downscaled SM estimates could be useful for enhancing the temporal and the spatial coverage of the dataset at the cost of a slightly higher ubRMSD. The following step could be the use of an ensemble of averaged downscaled SM data using geostationary satellites as MSG SEVIRI, which provide LST observations at a higher temporal resolution. Nevertheless, its applicability to an operational SM disaggregation algorithm requires more time and a higher computation capacity than the use of the averaged ensemble from MODIS.

Acknowledgements

This work was supported by the Spanish Ministry of Economy and Competitiveness, through a Formación Personal Investigador (FPI) grant BES-2011-043322, the project PROMISES: ESP2015-67549-C3, ERDF (European Regional Development Fund) and the BBVA foundation.

References

Anderson M.C., Norman J.M., Diak G.R., Kustas W.P., Mecikalski J.R. (1997) - *A two-source time-integrated model for estimating surface fluxes using thermal infrared remote sensing*. Remote Sensing of Environment, 60 (2): 195-216. doi: http://dx.doi.org/10.1016/S0034-4257(96)00215-5.

Anderson M.C., Norman J.M., Mecikalski J.R., Otkin J.A., Kustas W.P. (2007) - *A climatological study of evapotranspiration and moisture stress across the continental United States based on thermal remote sensing: 1. Model formulation*. Journal of Geophysical Research, 112 (D10): 1-7. doi: http://dx.doi.org/10.1029/2006JD007506.

Aminou D.M.A., Jaquet B., Pasternak F. (1997) - *Characteristics of the Meteosat Second Generation Radiometer/Imager: SEVIRI*. Proceedings of Society of Photo-optical Instrumentation Engineers, 3221: 19-31. doi: http://dx.doi.org/10.1117/12.298084.

BEC Team (2015) - *SMOS-BEC Ocean and Land Products Description*. Technical Report, Barcelona, Spain Available online at: http://cp34-bec.cmima.csic.es/doc/BEC-SMOS-

0001-PD.pdf.

Bruscantini C.A., Grings F.M., Barber M., Franco M., Entekhabi D., Karszenbaum H. (2015) - *A novel downscaling methodology for intermediate resolution radiometer data for SMAP*. IEEE International Geoscience and Remote Sensing Symposium, 1972-1975. doi: http://dx.doi.org/10.1109/IGARSS.2015.7326183.

Carlson T.N., Gillies R.R., Perry E.M. (1994) - *A method to make use of thermal infrared temperature and NDVI measurements to infer surface soil water content and fractional vegetation cover*. Remote Sensing Reviews, 9 (1-2): 161-173. doi: http://dx.doi.org/10.1080/ 02757259409532220.

Carlson T.N. (2007) - *An Overview of the "Triangle Method" for Estimating Surface Evapotranspiration and Soil Moisture from Satellite Imagery*. Sensors, 7 (8): 1612-1629. doi: http://dx.doi.org/10.3390/s7081612.

Chan S.K., Bindlish R., O'Neill P.E., Njoku E., Jackson T.J., Colliander A., Chen F., Burgin M., Dunbar S., Piepmeier J., Yueh S., Entekhabi D., Cosh M.H., Caldwell T., Walker J., Wu X., Berg A., Rowlandson T., Pacheco A., McNairn H., Thibeault M., Martínez-Fernández J., González-Zamora A., Seyfried M., Bosch D., Starks P., Goodrich D. Prueger J., Palecki M., Small E.E., Zreda M., Calvet J.C., Crow W.T., Kerr Y.H. (2016) - *Assessment of the SMAP Passive Soil Moisture Product*. IEEE Transactions on Geoscience and Remote Sensing, 54 (8): 4994-5007. doi: http://dx.doi.org/10.1109/TGRS.2016.2561938.

Das N.N., Entekhabi D., Njoku E. (2011) - *Algorithm for merging SMAP radiometer and radar data for high resolution soil moisture retrieval*. IEEE Transactions on Geoscience and Remote Sensing, 49 (5): 1504-1512. doi: http://dx.doi.org/10.1109/TGRS.2010.2089526.

Das N.N., Entekhabi D., Njoku E.G., Shi J.J.C., Johnson J.T., Colliander A. (2014) - *Tests of the SMAP Combined Radar and Radiometer Algorithm Using Airborne Field Campaign Observations and Simulated Data*. IEEE Transactions on Geoscience and Remote Sensing, 52 (4): 2018-2018. doi: http://dx.doi.org/10.1109/TGRS.2013.2257605.

Entekhabi D., Njoku E.G., O'Neill P.E., Kellogg K.H., Crow W.T., Edelstein W.N., Entin J.K., Goodman S.D., Jackson T.J., Johnson J., Kimball J., Piepmeier J.R., Koster R.D., Martin N., McDonald K.C., Moghaddam M., Moran S., Reichle R., Shi J.-C., Spencer M.W., Thurman S.W., Leung T., Van Zyl J. (2010a) - *The Soil Moisture Active Passive (SMAP) mission*. Proceedings of the IEEE, 98 (5): 704-716. doi: http://dx.doi.org/10.1109/JPROC.2010.2043918.

Entekhabi D., Reichle R.H., Koster R.D., Crow W.T. (2010b) - *Performance Metrics for Soil Moisture Retrievals and Application Requirements*. Journal of Hydrometeorology, 11 (3): 832-840. doi: http://dx.doi.org/10.1175/2010JHM1223.1.

Entekhabi D., Yueh S., O'Neill P., Kellogg K., Allen A., Bindlish R., Brown M., Chan S., Colliander A., Crow W.T., Das N., De Lannoy G., Dunbar R.S., Edelstein W.N., Entin J.K., Escobar V., Goodman S.D., Jackson T.J., Jai B., Johnson J., Kim E., Kim S., Kimball J., Koster R.D., Leon A., McDonald K.C., Moghaddam M., Mohamed P., Moran S., Njoku E.G., Piepmeier J.R., Reichle R., Rogez F., Shi J.C., Spencer M.W., Thurman S.W., Tsang L., Van Zyl J., Weiss B., West R. (2014) - *SMAP Handbook*. JPL Publication, 400-1567, Jet Propulsion Laboratory, Pasadena, California, USA, http://smap.jpl.nasa.gov/system/internal_resources/details/original/ 178_SMAP_Handbook_

FINAL_1_JULY_2014_Web.pdf.

Fang B., Lakshmi V. (2014) - *Soil moisture at watershed scale: remote sensing techniques.* Journal of Hydrology, 516: 258-272. doi: http://dx.doi.org/10.1016/j.jhydrol.2013.12.008.

Font J., Camps A., Borges A., Martin-Neira M., Boutin J., Reul N., Kerr Y.H., Hahne A., Mecklenburg S. (2010) - *SMOS: The Challenging Sea Surface Salinity Measurement From Space*. Proceedings of the IEEE, 98 (5): 649-665. doi: http://dx.doi.org/10.1109/JPROC.2009.2033096.

GCOS (2010) - *Implementation Plan for the Global Observing System for Climate in support of the UNFCCC, GCOS-138 (GOOS-184, GTOS-76, WMO-TD/No. 1523)*. Available online at: https://www.wmo.int/pages/prog/gcos/Publications/gcos-138.pdf.

Gillies R.R., Carlson T.N. (1995) - *Thermal Remote Sensing of Surface Soil Water Content with Partial Vegetation Cover for Incorporation into Climate Models*. Journal of Applied Meteorology, 34 (4): 745-756. doi: http://dx.doi.org/10.1175/1520-0450(1995)034<0745:TRSOSS>2.0.CO;2.

González-Zamora A., Sánchez N., Martínez-Fernández J., Gumuzzio A., Piles M., Olmedo E. (2015) - *Long-term SMOS soil moisture products: A comprehensive evaluation across scales and methods in the Duero Basin (Spain)*. Physics and Chemistry of the Earth, Parts A/B/C, 83-84: 123-136. doi: http://dx.doi.org/10.1016/j.pce.2015.05.009.

Guo P., Shi J., Zhao T. (2013) - *A downscaling algorithm for combining radar and radiometer observations for SMAP soil moisture retrieval*. IEEE International Geoscience and Remote Sensing Symposium (IGARSS*)*, pp. 731-734. doi: http://dx.doi.org/10.1109/IGARSS.2013.6721261.

IPCC (2014) - *Climate Change 2014: Synthesis Report*. Contribution of Working Groups I, II and III to the Fifth Assessment Report of the Intergovernmental Panel on Climate Change, Geneva, Switzerland.

Kerr Y.H., Waldteufel P., Wigneron J.-P., Delwart S., Cabot F., Boutin J., Escorihuela M.-J., Font J., Reul N., Gruhier C., Juglea S.E., Drinkwater M.R., Hahne A., Martin-Neira M., Mecklenburg S. (2010) - *The SMOS Mission: New Tool for Monitoring Key Elements of the Global Water Cycle*. Proceedings of the IEEE, 98 (5): 666-687. doi: http://dx.doi.org/10.1109/JPROC.2010.2043032.

Kerr Y.H., Al-Yaari A., Rodriguez-Fernandez N., Parrens M., Molero B., Leroux D., Bircher S., Mahmoodi A., Mialon A., Richaume P., Delwart S., Al Bitar A., Pellarin T., Bindlish R., Jackson T.J., Rüdiger C., Waldteufel P., Mecklenburg S., Wigneron J.-P. (2016) - *Overview of SMOS performance in terms of global soil moisture monitoring after six years in operation*. Remote Sensing of Environment, 180: 40-63. doi: http://dx.doi.org/10.1016/j.rse.2016.02.042.

Leone D. (2015) - *NASA Focused on Sentinel as Replacement for SMAP Radar*. Space News. Available online at: http://spacenews.com/nasa-focused-on-sentinel-as-replacement-for-smap-radar.

Martínez-Fernández J., Ceballos A. (2003) - *Temporal Stability of Soil Moisture in a Large-Field Experiment in Spain*. Soil Science Society of America Journal, 67 (6): 1647-1656. doi: http://dx.doi.org/10.2136/sssaj2003.1647.

Masson V., Champeau J.-L., Chauvin F., Meriguet C., Lacaze R. (2003) - *A global data base of land surface parameters at 1 km resolution in meteorological and climate*

models. Journal of Climate, 16 (9): 1261-1282. doi: http://dx.doi.org/10.1175/1520-0442-16.9.1261.

McMullan K.D., Brown M.A., Martin-Neira M., Rits W., Ekholm S., Marti J., Lemanczyk J. (2008) - *SMOS: The Payload*. IEEE Transactions in Geoscience and Remote Sensing, 46 (3): 594-605. doi: http://dx.doi.org/10.1109/TGRS.2007.914809.

Merlin O., Rudiger C., Al Bitar A., Richaume P., Walker J.P., Kerr Y.H. (2012) - *Disaggregation of SMOS Soil Moisture in Southeastern Australia.* IEEE Transactions on Geoscience and Remote Sensing, 50 (5): 1556-1571. doi: http://dx.doi.org/10.1109/TGRS.2011.2175000.

Moran M.S., Clarke T.R., Inoue Y., Vidal A. (1994) - *Estimating crop water deficit using the relation between surface-air temperature and spectral vegetation index*. Remote Sensing of Environment, 49 (3): 246-263. doi: http://dx.doi.org/10.1016/0034-4257(94)90020-5.

Ochsner T.E., Cosh M.H., Cuenca R.H., Dorigo W.A., Draper C.S., Hagimoto Y., Kerr Y.H., Njoku E.G., Small E.E., Zreda M. (2013) - *State of the art in large-scale soil moisture monitoring*. Soil Science Society of America Journal, 77 (6): 1888-1919. doi: http://dx.doi.org/10.2136/sssaj2013.03.0093.

Pablos M., Piles M., Sánchez N., Gonzalez-Gambau V., Vall-llossera M., Camps A., Martínez-Fernandez J. (2014) - *A sensitivity study of land surface temperature to soil moisture using in-situ and spaceborne observations*. IEEE International Geoscience on Remote Sensing Symphosium, pp. 3267-3269. doi: http://dx.doi.org/10.1109/IGARSS.2014.6947176.

Pablos M., Martínez-Fernández J., Piles M., Sánchez N., Vall-llossera M., Camps A. (2016) - *Multi-temporal evaluation of soil moisture and land surface temperature dynamics using in situ and satellite observations*. Remote Sensing, 8 (7): 587. doi: http://dx.doi.org/10.3390/ rs8070587.

Petropoulos G.P., Carlson T.N., Wooster M.J., Islam S. (2009) - *A review of Ts/VI remote sensing based methods for the retrieval of land surface energy fluxes and soil moisture*. Progress in Physical Geography, 33 (2): 224-250. doi: http://dx.doi.org/10.1177/0309133309338997.

Piles M., Entekhabi D., Camps A. (2009) - *A Change Detection Algorithm for Retrieving High-Resolution Soil Moisture From SMAP Radar and Radiometer Observations*. IEEE Transactions on Geoscience and Remote Sensing, 47 (12): 4125-4131. doi: http://dx.doi.org/10.1109/TGRS.2009.2022088.

Piles M., Camps A., Vall-Llossera M., Corbella I., Panciera R., Rudiger C., Kerr Y.H., Walker J. (2011) - *Downscaling SMOS-derived soil moisture using MODIS visible/infrared data.* IEEE Transactions on Geoscience and Remote Sensing, 49 (9): 3156-3166. doi: http://dx.doi.org/10.1109/TGRS.2011.2120615.

Piles M., Vall-llossera M., Laguna L., Camps A. (2012) - *A downscaling approach to combine SMOS multi-angular and full-polarimetric observations with MODIS VIS/IR data into high resolution soil moisture maps*. IEEE International Geoscience and Remote Sensing Symposium (IGARSS), pp. 1247-1250. doi: http://dx.doi.org/10.1109/IGARSS.2012.6351316.

Piles M., Sánchez N., Vall-llossera M., Camps A., Martínez-Fernandez J., Martínez J., González-Gambau V. (2014) - *A Downscaling Approach for SMOS Land Observations: Evaluation of High-Resolution Soil Moisture Maps Over the Iberian Peninsula*. IEEE

Journal of Selected Topics in Applied Earth Observations and Remote Sensing, 7 (9): 845-3857. doi: http://dx.doi.org/10.1109/JSTARS.2014.2325398.

Piles M., Sánchez N. (2016) - *Spatial downscaling of passive microwave data with visible-to-infrared information for high-resolution soil moisture mapping*. Chapter of: Satellite Soil Moisture Retrieval: Techniques and Applications, Srivastava P.K, Petropoulos G., Kerr Y.H. (Eds.), Elsevier.

Piles M., Petropoulos G.P., Sánchez N., González-Zamora A., Ireland G. (2016) - *Towards improved spatio-temporal resolution soil moisture retrievals from the synergy of SMOS and MSG SEVIRI spaceborne observations*. Remote Sensing of Environment, 180: 403-417. doi: http://dx.doi.org/10.1016/j.rse.2016.02.048.

Price J.C. (1980) - *The potential of remotely sensed thermal infrared data to infer surface soil moisture and evaporation*. Water Resources Research, 16 (4): 787-795. doi: http://dx.doi.org/10.1029/WR016i004p00787.

Sánchez N., Martínez-Fernández J., Scaini A., Pérez-Gutiérrez C. (2012) - *Validation of the SMOS L2 soil moisture data in the REMEDHUS network (Spain)*. IEEE Transactions on Geoscience and Remote Sensing, 50 (5): 1602-1611. doi: http://dx.doi.org/10.1109/TGRS.2012.2186971.

Sánchez-Ruiz S., Piles M., Sánchez N., Martínez-Fernández J., Vall-llossera M., Camps A. (2014) - *Combining SMOS with visible and near/shortwave/thermal infrared satellite data for high resolution soil moisture estimates*. Journal of Hydrology, 49: 3156-3166. doi: http://dx.doi.org/10.1016/j.jhydrol.2013.12.047.

Sandholt I., Rasmussen K., Andersen J. (2002) - *A simple interpretation of the surface temperature/vegetation index space for assessment of surface moisture status*. Remote Sensing of Environment, 79 (2-3): 213-224. doi: http://dx.doi.org/10.1016/S0034-4257(01)00274-7.

Seneviratne S.I., Corti T., Davin E.L., Hirschi M., Jaeger E.B., Lehner I., Orlowsky B., Teuling A.J. (2010) - *Investigating soil moisture-climate interactions in a changing climate: A review*. Earth-Science Reviews, 99: 125-161.

Song C., Jia L. (2013) - *An improved method for downscaling soil moisture retrieved by SMOS with MODIS LST/NDVI*. IEEE International Geoscience and Remote Sensing Symposium (IGARSS), pp. 2696-2699. doi: http://dx.doi.org/10.1109/IGARSS.2013.6723379.

Stisen S., Sandholt I., Norgaard A., Fensholt R., Jensen R.K. (2008) - *Combining the triangle method with thermal inertia to estimate regional evapotranspiration - Applied to MSG-SEVIRI data in the Senegal River basin*. Remote Sensing of Environment, 112 (3): 1242-1255. doi: http://dx.doi.org/10.1016/j.rse.2007.08.013.

Wan Z., Snyder W. (1999) - *MODIS land-surface temperature algorithm theoretical basis document version 3.3*. Institute for Computational Earth System Science, University of California, USA.